Reduction of Thermal Fluctuations in a Cryogenic Laser Interferometric Gravitational Wave Detector

Takashi Uchiyama,[1,*] Shinji Miyoki,[2] Souichi Telada,[3] Kazuhiro Yamamoto,[4,†] Masatake Ohashi,[2]
Kazuhiro Agatsuma,[2,‡] Koji Arai,[5,§] Masa-Katsu Fujimoto,[5] Tomiyoshi Haruyama,[6] Seiji Kawamura,[5,†]
Osamu Miyakawa,[1] Naoko Ohishi,[1,‡] Takanori Saito,[2] Takakazu Shintomi,[7] Toshikazu Suzuki,[6]
Ryutaro Takahashi,[5,†] and Daisuke Tatsumi[5]

[1]*Kamioka Observatory, Institute for Cosmic Ray Research, The University of Tokyo,
456 Higashi-Mozumi, Kamioka, Hida Gifu 506-1205, Japan*
[2]*Institute for Cosmic Ray Research, The University of Tokyo, 5-1-5 Kashiwa-no-ha, Kashiwa, Chiba 277-8582, Japan*
[3]*National Institute of Advanced Industrial Science and Technology, 1-1-1 Umezono, Tsukuba, Ibaraki 305-8568, Japan*
[4]*Max-Planck-Institut für Gravitationsphysik (Albert-Einstein-Institut) and Institut für Gravitationsphysik,
Leibniz Universität Hannover, Callinstrasse 38, D-30167 Hannover, Germany*
[5]*National Astronomical Observatory of Japan, 2-21-1 Osawa, Mitaka, Tokyo 181-8588, Japan*
[6]*High Energy Accelerator Research Organization, KEK, 1-1 Oho, Tsukuba, Ibaraki 305-0801, Japan*
[7]*Advanced Research Institute for the Sciences and Humanities, Nihon University, 12-5 Goban-cho, Chiyoda-ku,
Tokyo 102-8251, Japan*

The thermal fluctuation of mirror surfaces is the fundamental limitation for interferometric gravitational wave (GW) detectors. Here, we experimentally demonstrate for the first time a reduction in a mirror's thermal fluctuation in a GW detector with sapphire mirrors from the Cryogenic Laser Interferometer Observatory at 17 and 18 K. The detector sensitivity, which was limited by the mirror's thermal fluctuation at room temperature, was improved in the frequency range of 90 to 240 Hz by cooling the mirrors. The improved sensitivity reached a maximum of 2.2×10^{-19} m/$\sqrt{\text{Hz}}$ at 165 Hz.

Introduction.—Two hundred years ago, Robert Brown investigated the random motion of small particles in water [1]. This random motion is now understood to be an irreducible natural phenomenon, and it creates a fundamental limit on the precision of measurements, including the measurement of fundamental constants, high-resolution spectroscopy and fundamental physics experiments using a frequency-stabilized laser [2] and gravitational wave (GW) detection by a laser interferometer with suspended mirrors [3].

In the case of interferometric GW detectors, thermal noise in the mirror typically limits the detector sensitivity to approximately a few hundred Hz, which lies in the important frequency region for the detection of GWs from the binary coalescence of neutron stars. Although kilometer-scale first-generation laser interferometric GW detectors, such as the Laser Interferometer Gravitational-Wave Observatory (LIGO) [4] and VIRGO [5], have already performed several long-term observation runs, no GW signal has yet been observed. The sensitivity must be improved by 1 order of magnitude to be able to detect GWs within a single year of observation.

According to the fluctuation-dissipation theorem [6], the power of thermal fluctuations is proportional to both temperature and mechanical loss. Thus, a mirror constructed of a low-loss material operating at a cryogenic temperature (a cryogenic mirror) is a good candidate for creating a low-thermal-fluctuation mirror. Because of various difficulties associated with implementing cryogenic mirrors in interferometers, major effort has thus far been devoted to finding low-loss materials at room temperature.

We originally proposed using a suspended sapphire mirror cooled to less than 20 K for a GW detector [7], and we have researched and developed this technique [8–15]. Here, we demonstrate for the first time a reduction in mirror thermal fluctuations using this cryogenic mirror in a working GW detector. This reduction is the primary purpose of the Cryogenic Laser Interferometer Observatory (CLIO) [16], which is the first GW detector to use a cryogenic mirror.

Experiment.—CLIO was built at an underground site in the Kamioka mine, which is located 220 km northwest of Tokyo in Japan. CLIO is a Michelson interferometer with 100-m Fabry-Perot (FP) arm cavities, each consisting of front and end mirrors [16,17]. The front mirrors are suspended closest to the beam splitter and were cooled to 17 and 18 K for the sensitivity measurement reported in this study. The end mirrors remained at 299 K.

The cavity mirror substrate material is sapphire. The cylindrical substrate has a diameter of 100 mm, a thickness of 60 mm, and a mass of 1.8 kg. One surface of the substrate has a highly reflective multilayered film coating of SiO_2 and Ta_2O_5. The mirror is suspended at the final stage of a six-stage suspension system [18], and the length of the wire suspending the mirror is 400 mm.

The suspension system is installed in a cryostat with two layers of radiation shielding (an outer and an inner shield) [18]. A two-stage pulse-tube cryocooler [19] cools the outer and inner shields to approximately 70 and 10 K, respectively. It took approximately 250 hours to cool the mirrors, and the vacuum pressure was less than 10^{-4} Pa.

To cool the front mirrors, we changed the mirror suspension wires from Bolfur to 99.999% purity aluminum to provide higher thermal conductivity, and we added three heat links to each suspension system [17]. Bolfur wire is an amorphous metal wire made by Unitika, Ltd. with a diameter of 50 μm. The aluminum wire used has a diameter of 0.5 mm. The same aluminum wire was used for the heat links, which provide thermal conduction between the suspended masses (damping stage, cryobase, and upper mass) and the inner shield in the cryostat [18]. The lengths of the heat links between the inner shield and the cryobase, between the cryobase and the upper mass and between the damping stage and the inner shield were 315 mm, 115 mm and 150 mm, respectively; each had one heat link. Thermometers were attached to the cryobase and the upper mass. We estimated the temperature of the mirror from the temperatures of the cryobase and the upper mass and from the thermal conductivity of the mirror suspension wires and the heat link.

One 100-m FP cavity serves as a reference for the laser frequency stabilization, and the length of the other 100-m FP cavity is controlled to maintain the optical resonance [16]. Coil-magnet actuators, consisting of magnets glued to the mirror and coils facing toward the magnets, are used to control the cavity length. The GW signal is included in the feedback signal for this length control. In this study, the sensitivity was characterized by the power spectrum density of the displacement in units of m/$\sqrt{\text{Hz}}$ and is calculated using the following three measurements: the feedback signal, V/$\sqrt{\text{Hz}}$, the loop gain of the length control system, and the response function of the coil-magnet actuators, m/V.

The thermal fluctuation of a mirror surface is caused by several different loss mechanisms. The thermoelastic damping and the internal frictional loss of the sapphire substrate and of the reflective coating films were considered in this study. In the case of the sapphire mirror at room temperature, the largest loss mechanism is the thermoelastic damping of the sapphire substrate (thermoelastic noise). At temperatures below 20 K, the internal frictional loss of the reflective coating films is expected to be the largest loss mechanism.

The theory of thermoelastic noise [20,21] has previously been validated experimentally [22]. The power spectrum density (m^2/Hz) of the thermoelastic noise in a mirror was shown in Black *et al.* [22] and described as follows:

$$S_{\text{TE}}(\omega) = \frac{4}{\sqrt{\pi}} \frac{\alpha^2 (1 + \sigma)^2}{\kappa} k_B T^2 W J(\Omega), \quad (1)$$

where $J(\Omega)$ is

$$J(\Omega) = \frac{\sqrt{2}}{\pi^{3/2}} \int_0^\infty du \int_{-\infty}^{+\infty} dv \frac{u^3 e^{-u^2/2}}{(u^2 + v^2)[(u^2 + v^2)^2 + \Omega^2]}, \quad (2)$$

and Ω is

$$\Omega = \frac{\omega}{\omega_c}, \quad (3)$$

where ω_c is

$$\omega_c = \frac{2\kappa}{\rho C W^2}. \quad (4)$$

In these equations, ω is the angular frequency, α is the thermal expansion coefficient, σ is the Poisson's ratio, κ is the thermal conductivity, ρC is the specific heat per unit volume, k_B is the Boltzmann constant, T is the temperature of the mirror, and W is the beam spot radius on the mirror. In the case of the CLIO mirror at room temperature, $\Omega \gg 1$ is satisfied near 100 Hz. In this case, the power spectrum density (m^2/Hz) is simplified as follows:

$$S_{\text{TE}}^{\Omega \gg 1}(\omega) = \frac{16}{\sqrt{\pi}} \alpha^2 (1 + \sigma)^2 \frac{k_B T^2 \kappa}{(\omega \rho C)^2} \frac{1}{W^3}. \quad (5)$$

The power spectrum density (m^2/Hz) of the thermal noise in a mirror caused by the internal frictional loss of the substrate and of the coating films was shown in Nakagawa *et al.* [23] as follows:

$$S(f) = \frac{2 k_B T (1 - \sigma^2)}{\pi^{3/2} f W E} \phi_{\text{substr}}$$
$$\times \left\{ 1 + \frac{2}{\sqrt{\pi}} \frac{(1 - 2\sigma)}{(1 - \sigma)} \frac{\phi_{\text{coat}}}{\phi_{\text{substr}}} \left(\frac{d}{W} \right) \right\}. \quad (6)$$

In this equation, E is the Young's modulus, d is the thickness of the coating films, and ϕ_{substr} and ϕ_{coat} are the internal frictional loss of the substrate and of the coating films, respectively.

Results.—For comparison, Fig. 1 presents both the displacement sensitivity curve measured with the front CLIO mirrors cooled to 17 and 18 K (cryogenic sensitivity; CryoSens) as well as the curve without cooled mirrors (room-temperature sensitivity; RoomSens). CryoSens and RoomSens were measured on March 20, 2010 and November 5, 2008, respectively. The loop gain of the length control was measured immediately after each feedback signal measurement, and the response function of the coil-magnet actuators was calibrated for each experimental configuration. A sensitivity curve consists of frequency-dependent noise floors and multiple line noises. The noise-floor level of CryoSens from 90 Hz to 240 Hz is below the noise-floor level of RoomSens. By reducing this noise-floor level, the detection range for GW signals from the binary coalescence of neutron stars in the optimal direction was improved from 150 kpc to 160 kpc. The noise
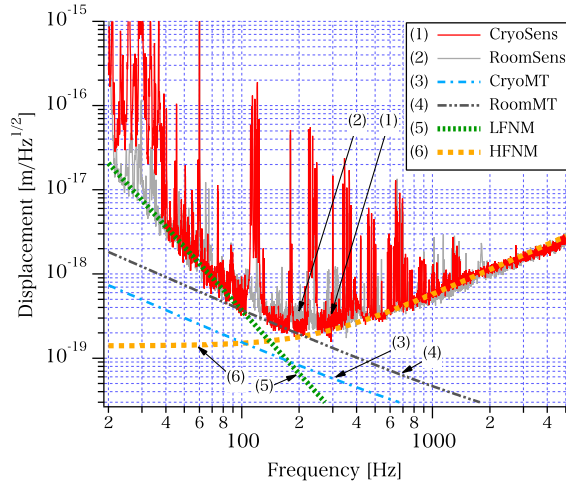
FIG. 1 (color online). Comparison of CLIO displacement sensitivity curves. Cryogenic sensitivity (CryoSens) was measured with the front mirrors at 17 and 18 K and with the end mirrors at room temperature (299 K). Room-temperature sensitivity (RoomSens) was measured with all of the mirrors at 299 K. CryoSens and RoomSens were measured on March 20, 2010 and November 5, 2008, respectively. The magnified sensitivity curves are shown in Fig. 2. Mirror thermal noise estimate curves corresponding to each of the sensitivity measurements are also shown (CryoMT and RoomMT). The CryoMT and the RoomMT were estimated to be 1.5×10^{-19} m/$\sqrt{\text{Hz}} \times (100 \text{ Hz}/f)$ and 3.7×10^{-19} m/$\sqrt{\text{Hz}} \times (100 \text{ Hz}/f)$, respectively. The low-frequency noise model (LFNM) consists of the fitted lines for the noise-floor level of CryoSens from 40 Hz to 70 Hz and for RoomSens from 20 Hz to 70 Hz. The LFNM was estimated to be 3.7×10^{-19} m/$\sqrt{\text{Hz}} \times (100 \text{ Hz}/f)^{2.5}$. The high-frequency noise model (HFNM) consists of the fitted lines for the noise-floor levels of both sensitivity curves above 400 Hz. Based on the characteristics of the 100-m Fabry-Perot cavities of CLIO, the HFNM was found to be 1.4×10^{-19} m/$\sqrt{\text{Hz}} \times \sqrt{1 + (f/250 \text{ Hz})^2}$.

floor at 165 Hz was reduced from 3.1×10^{-19} m/$\sqrt{\text{Hz}}$ to 2.2×10^{-19} m/$\sqrt{\text{Hz}}$ by cooling the front mirrors.

Discussion.—The noise floors of the two sensitivities shown in Fig. 1 are very similar from 40 Hz to 90 Hz and from 400 Hz to 5 kHz, although additional line noises appeared in CryoSens. The line noise near 30 Hz results from the mechanical resonance of the cooled front mirror suspension systems. The line noise near 120 Hz and its higher-order harmonics are also caused by mechanical resonance in the suspension wires of the cooled front mirrors. The line noise at 60 Hz and its higher harmonics are similar to electric power line noise.

Figure 1 also shows the mirror thermal noise estimates corresponding to each sensitivity measurement (CryoMT and RoomMT), with the fitted lines for the noise floor in the low-frequency region (the low-frequency noise model; LFNM) and the high-frequency region (the high-frequency noise model; HFNM).

The parameters for the thermal noise calculation are summarized in Table I. We did not perform any fits to the parameters. The RoomMT was calculated to be 3.7×10^{-19} m/$\sqrt{\text{Hz}} \times (100 \text{ Hz}/f)$. Because the mirror thermal noise is larger with a smaller laser beam, the thermal noise of the front mirror is approximately twice as large as the thermal noise of the end mirror in the RoomMT. The CryoMT was greatly reduced to 1.5×10^{-19} m/$\sqrt{\text{Hz}} \times (100 \text{ Hz}/f)$ by the decrease in the thermal fluctuation of the cooled front mirrors. If all CLIO mirrors are cooled to 20 K, the mirror thermal noise near 100 Hz should be reduced to 1.7×10^{-20} m/$\sqrt{\text{Hz}} \times (100 \text{ Hz}/f)^{1/2}$.

The LFNM was estimated from the noise floor of CryoSens between 40 and 70 Hz and the noise floor of RoomSens between 20 and 70 Hz, with a value of 3.7×10^{-19} m/$\sqrt{\text{Hz}} \times (100 \text{ Hz}/f)^{2.5}$. A discussion of

TABLE I. Parameters for sapphire mirror thermal noise estimation

	Objects	Unit	Room temperature	Cryogenic
	Mirror temperature	K	299	17 and 18
W_{front}	Beam spot radius on front mirrors	mm	4.9	4.9
W_{end}	Beam spot radius on end mirrors	mm	8.5	8.5
	Material properties of Sapphire			
α	Thermal expansion coefficient [24,25]	1/K	5.4×10^{-6}	5.6×10^{-9}
ρC	Specific heat per unit volume [24]	J/K/m^3	3.1×10^{6}	2.8×10^{3}
κ	Thermal conductivity [24]	W/m/K	46	1.6×10^{4}
σ	Poisson's ratio[a]		0.27	0.27
E	Young's modulus [10]	Pa	40×10^{10}	40×10^{10}
ϕ_{substr}	Mechanical loss [8]		$1/4.6 \times 10^{6}$	$1/1.5 \times 10^{8}$
ϕ_{coat}	Mechanical loss in coating films [10]		4.0×10^{-4}	4.0×10^{-4}
d	Thickness of coating films	μm	3.9	3.9

[a]We found various values for the Poisson's ratio of sapphire between 0.23 and 0.30. We used the averaged value.

the origin of the LFNM is outside the scope of the current work. The HFNM was estimated from the noise floors of both sensitivity curves above 400 Hz by assuming a simple pole frequency dependence [26]. The HFNM consists of photocurrent shot noise and laser intensity noise at a frequency of 15.8 MHz and was estimated to have a value of 1.4×10^{-19} m/$\sqrt{\text{Hz}} \times \sqrt{1 + (f/250 \text{ Hz})^2}$; the HFNM depends on the length and finesse of the 100-m FP cavity. Cavity pole frequencies of 262 and 246 Hz were obtained for the measurements of CryoSens and RoomSens, respectively. The systematic error in the noise-floor amplitude due to the discrepancy in the cavity pole frequencies was less than 2% at frequency below 200 Hz.

Figure 2 compares CryoSens, RoomSens, the cryogenic noise model (CryoNM), and the room-temperature noise model (RoomNM). CryoNM is the quadrature sum of the LFNM, the HFNM, and CryoMT. RoomNM is the quadrature sum of the LFNM, the HFNM, and RoomMT. Error bars are shown for both CryoNM and RoomNM, representing the quadrature sum of the calibration error and the

noise estimation error. We estimated a $\pm 2.5\%$ systematic error for the calibration, a $\pm 5\%$ estimation error for CryoMT and RoomMT, and a $\pm 10\%$ statistical error for LFNM and HFNM. The noise estimation error is the quadrature sum of the error in the mirror thermal noise estimate (CryoMT or RoomMT) and the errors in LFNM and HFNM.

The noise floor of RoomSens agrees with RoomNM. The noise floor of CryoSens is below RoomNM and agrees instead with CryoNM. The difference between CryoNM and RoomNM is solely based on the mirror thermal noise estimate. Thus, we conclude that the sensitivity limitation due to thermal noise in the mirror at room temperature was improved by the noise reduction because of the decreased thermal fluctuation in the cooled front mirrors. This observation is the first demonstration that mirrors display less thermal fluctuation at cryogenic temperatures than at room temperature.

Conclusion.—The thermal fluctuation of mirror surfaces represents the fundamental limitation on experiments that require high-precision measurements, such as experiments using a frequency-stabilized laser and GW detection using a laser interferometer. The cryogenic mirror technique uses a low-mechanical-loss mirror at a low temperature to reduce such fluctuations. Our demonstration using an actual GW detector directly proves that the cryogenic mirror technique effectively improves the sensitivity of the GW detector. This cryogenic mirror technique will be used in advanced GW detectors, such as KAGRA formerly called the Large-Scale Cryogenic Gravitational Wave Telescope [27], on which construction began in the middle of 2010 in Japan, and the Einstein Telescope project in Europe [28]. The mirror thermal noise of KAGRA near 100 Hz, which limits the sensitivity to 4×10^{-20} m/$\sqrt{\text{Hz}} \times (100 \text{ Hz}/f)$ at 299 K, will be reduced to 5×10^{-21} m/$\sqrt{\text{Hz}} \times (100 \text{ Hz}/f)^{1/2}$ at 20 K due to the cryogenic mirror technique. The KAGRA sensitivity will make it possible to detect a GW signal from the binary coalescence of neutron stars in the optimal direction up to 250 Mpc with a signal-to-noise ratio of 10 and the event rate is expected to be approximately 6 events per year [27]. We believe that our achievement represents a breakthrough in the study of thermal fluctuations, laser frequency stabilization, and GW detection.
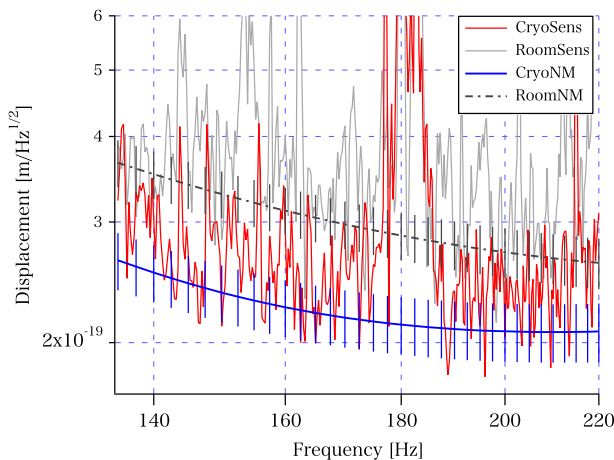
FIG. 2 (color online). Comparison of CLIO displacement sensitivity curves and noise models. The cryogenic sensitivity (CryoSens) and the room-temperature sensitivity (RoomSens) show similar curves, as observed in Fig. 1. The cryogenic noise model (CryoNM) is the noise-floor model curve for CryoSens and is calculated as the quadrature sum of the low-frequency noise model (LFNM), the high-frequency noise model (HFNM), and the mirror thermal noise estimate for CryoSens (CryoMT). The room-temperature noise model (RoomNM) is the noise-floor model curve for RoomSens and is calculated as the quadrature sum of the LFNM, the HFNM, and the mirror thermal noise estimate for RoomSens (RoomMT). Error bars are shown for both CryoNM and RoomNM, representing the quadrature sums of the calibration error and the noise estimation errors. We estimated a systematic calibration error of $\pm 2.5\%$, a $\pm 5\%$ estimation error for CryoMT and RoomMT, and a $\pm 10\%$ statistical error for LFNM and HFNM. The noise estimation error is the quadrature sum of the error in the mirror thermal noise estimate (CryoMT or RoomMT) and the errors in the LFNM and HFNM.

*uchiyama@icrr.u-tokyo.ac.jp

†Present address: Institute for Cosmic Ray Research, the University of Tokyo, 5-1-5 Kashiwa-no-ha, Kashiwa, Chiba 277-8582, Japan.

‡Present address: National Astronomical Observatory of Japan, 2-21-1 Osawa, Mitaka, Tokyo 181-8588, Japan.

§Present address: LIGO project, California Institute of Technology 100-36, Pasadena, CA 91125, USA.

[1] R. Brown, Philos. Mag. **4**, 161 (1828).

[2] K. Numata, A. Kemery, and J. Camp, Phys. Rev. Lett. **93**, 250602 (2004).

[3] P. R. Saulson, Phys. Rev. D **42**, 2437 (1990).

[4] A. Abramovici et al., Science **256**, 325 (1992).

[5] C. Bradaschia et al., Nucl. Instrum. Methods Phys. Res., Sect. A **289**, 518 (1990).

[6] H. B. Callen and T. A. Welton, Phys. Rev. **83**, 34 (1951).

[7] T. Uchiyama, D. Tatsumi, T. Tomaru, M. E. Tobar, K. Kuroda, T. Suzuki, N. Sato, A. Yamamoto, T. Haruyama, and T. Shintomi, Phys. Lett. A **242**, 211 (1998).

[8] T. Uchiyama et al., Phys. Lett. A **261**, 5 (1999).

[9] T. Uchiyama, T. Tomaru, D Tatsumi, S. Miyoki, M. Ohashi, K. Kuroda, T. Suzuki, A. Yamamoto, and T. Shintomi, Phys. Lett. A **273**, 310 (2000).

[10] K. Yamamoto et al., Phys. Rev. D **74**, 022002 (2006).

[11] T. Tomaru, T. Suzuki, T. Uchiyama, A. Yamamoto, T. Shintomi, C. T. Taylor, K. Yamamoto, S. Miyoki, M. Ohashi, and K. Kuroda, Phys. Lett. A **301**, 215 (2002).

[12] T. Tomaru, T. Uchiyama, D. Tatsumi, S. Miyoki, M. Ohashi, K. Kuroda, T. Suzuki, A. Yamamoto, and T. Shintomi, Phys. Lett. A **283**, 80 (2001).

[13] S. Miyoki et al., Cryogenics **41**, 415 (2001).

[14] M. Ohashi et al., Classical Quantum Gravity **20**, S599 (2003).

[15] T. Tomaru, T. Suzuki, S. Miyoki, T. Uchiyama, C. T. Taylor, A. Yamamoto, T. Shintomi, M. Ohashi and K. Kuroda, Classical Quantum Gravity **19**, 2045 (2002).

[16] K. Agatsuma et al., Classical Quantum Gravity **27**, 084022 (2010).

[17] K. Yamamoto et al., J. Phys. Conf. Ser. **122**, 012002 (2008).

[18] T. Uchiyama et al., J. Phys. Conf. Ser. **32**, 259 (2006).

[19] Y. Ikushima, R. Li, T. Tomaru, N. Sato, T. Suzuki, T. Haruyama, T. Shintomi, and A. Yamamoto, Cryogenics **48**, 406 (2008).

[20] V. B. Braginsky, M. L. Gorodetsky, and S. P. Vyatchanin, Phys. Lett. A **264**, 1 (1999).

[21] M. Cerdonio, L. Conti, A. Heidmann, and M. Pinard, Phys. Rev. D **63**, 082003 (2001).

[22] E. D. Black, A. Villar, and K. G. Libbrecht, Phys. Rev. Lett. **93**, 241101 (2004).

[23] N. Nakagawa, A. M. Gretarsson, E. K. Gustafson, and M. M. Fejer, Phys. Rev. D **65**, 102001 (2002).

[24] Y. S. Touloukian, R. K. Kirby, E. R. Taylor, and T. Y. R. Lee, Thermophysical Properties of Matter—the TPRC Data Series (IFI/Plenum, New York, 1970).

[25] C. T. Taylor, M. Notcutt, E. K. Wong, A. G. Mann, and D. G. Blair, Opt. Commun. **131**, 311 (1996).

[26] P. R. Saulson, Fundamentals of Interferometric Gravitational Wave Detectors (World Scientific, Singapore, 1994).

[27] K. Kuroda et al., Classical Quantum Gravity **27**, 084004 (2010).

[28] M. Punturo et al., Classical Quantum Gravity **27**, 084007 (2010).